AIAA SPACE Forum
12 - 14 Sep 2017, Orlando, FL
AIAA SPACE and Astronautics Forum and Exposition

Design and Control of Growth Adaptable Artificial Gravity Space Habitats

Raman Goyal*, Tyler Bryant*, Manoranjan Majji†, Robert E. Skelton‡
Department of Aerospace Engineering, Texas A&M University, TX, USA
Anthony Longman§
Skyframe Research & Development Inc., Camarillo, CA, USA

We seek to solve 5 unsolved problems in space: Providing gravity, food, radiation protection, and a growable technology that enlarges the habitat as economics allow. A *full-scale* center for space research is needed to keep the gravity gradient across the human body less than 6%, to avoid nausea and other health issues. The artificial gravity is provided by centripetal forces in a spinning habitat. The agricultural space occupies the low gravity part of the habitat. The radiation protection requires 5m of regolith from ISRU. The habitat will be roomy and research can determine the level of gravity required for human health, as ONLY a large space habitat can do (the plan grows to 225m radius yielding only 1% gravity gradient). The tensegrity paradigm is used for the design of the growth adaptable space structure. The mass required to sustain the centrifugal forces and the atmospheric pressure is minimized using the tensegrity structural paradigm. The transient dynamics of the structure during pressurization is shown. The growth strategy is planned for continuous occupancy of humans and agriculture. A control scheme is provided to stabilize the sun-pointing attitude, while spinning at a desired rate for artificial gravity. Numerical simulations are used to demonstrate the efficacy of the control laws for the space habitat system.

Nomenclature

N	Node Matrix
W	External force Matrix
C_s	Connectivity Matrix
γ	Force density in the string, N/m
S	String vectors Matrix
ρ	Density, kg/m^3
σ	Yield strength, N/m^2
Θ	Direction Cosine Matrix
$\overline{\omega}$	Desired Angular Velocity Vector
$\underline{\omega}$	Actual Angular Velocity Vector
$\underline{e_\omega}$	Error in Angular Velocity
$\overline{J}$	Moment of Inertia, kg-m^2
T	Torque, N-m
Ω_2	Angular velocity to get required gravity at the surface, rad/sec
Ω_3	Angular velocity (360 degrees/year) to follow the sun, rad/sec

Subscript

*Graduate Student, Department of Aerospace Engineering, Texas A&M University, and AIAA Student Member.
†Assistant Professor, Department of Aerospace Engineering, Texas A&M University, and AIAA Senior Member.
‡TEES Distinguished Research Professor, Department of Aerospace Engineering, Texas A&M University, and AIAA Emeritus Member.
§Chief Designer & CEO, Skyframe Research & Development Inc., Camarillo, CA, 2013 NIAC Fellow, AIAA Associate.

i Variable number

I. Introduction

The USA has been in space for over 50 years in zero-g, and it is unhealthy. This project shows the feasibility of artificial gravity (AG) in space while providing habitat growth adaptability, radiation protection, and agricultural space. There have been numerous studies showing the detrimental effects on the health of astronauts due to the absence of gravitational field in space. Problems like bone density loss, impaired vision, muscle atrophy, cardiovascular deconditioning and immune system change are prevalent in astronauts after spending considerable time in space.[1–4] Various researchers have proposed AG in space for human space exploration.[5–7] Projects like TransHab[8] were started by NASA to provide earth like gravitational pull for long journeys in space, but economics was a big deterrent and the problem still remains unsolved. We believe that a settlement in space, with research capabilities, is the most efficient path to solve the problems of long term presence of humans in space, including space travel. We need to know what level of gravity is required for human health, and we need to know that before launching long term space travel to Mars and further. We want an environment that allows children to grow normally.

Material resources are costly in space, so we must prove minimal mass concepts for our habitat structure. Tensegrity systems have been shown to produce minimal mass solutions to the five fundamental problems in engineering mechanics: What is the minimal mass structure in the presence of i) torsional loads, ii) simply-supported bending loads, iii) compressive loads, iv) cantilevered loads, and iv) tension loads. Tensegrity is a network of axially loaded prestressable members. This definition is given by Skelton,[9] but Fuller coined the word "Tensegrity" just to describe the work of Kenneth Snelson, namely a continuous network of tension members separated by a discontinuous network of compressive members,.[10,11] To differentiate between various types of tensegrity structures, Skelton defines a tensegrity configuration that has no contacts between its rigid bodies is a class 1 tensegrity system, and a tensegrity system with as many as k rigid bodies in contact is a class k tensegrity system.[9] The minimum mass solution for five fundamental engineering mechanics problem has been provided by tensegrity systems.[9,12–14] Furthermore, with tensegrity one can change the shape of structures without changing stiffness, and can change stiffness without changing shape. Tensegrity offers the space industry easy controllability and deployability.[15–19]

The goal of this project is to provide artificial gravity and growth strategy to a large spacious habitat as opposed to current limited space cubicles. Several design concepts can be analyzed to provide enough space for humans and to maintain a constant gravity throughout the surface of the habitat. Section (II) discusses several possible habitat configurations such as the bola, spiral, torus, and cylinder. Concentric cylinders were chosen as the design concept because of its easy fabrication, efficient use of space, and simple growth strategy. In section (III), we discuss the growth strategy by adding more concentric cylinders and expanding the shield to accommodate both people and agriculture life while maintaining a safe environment.

Section (IV) discusses the structural design of the cylinder membrane to optimize mass and provide the required stiffness. The dynamics of the structure are shown during inflation and sudden pressure change transients. Section (V) talks about the precession and attitude control of the habitat. Toward this end, we need to control the spin rate and direction of habitat to get enough sunlight and provide AG. We must satisfy three goals: spin the habitat to achieve $1g$ at the surface, spin the habitat about another axis to keep the precession and always point toward the sun (the axis of rotation is pointing toward the sun). Finally, section (VI) provides the conclusion with the forward direction of some planned future work.

II. Design Concepts

The following design concepts were studied to meet the need of spacious environment, easy growth and constant gravity.

A. Bola

A single cable could support a spacecraft on each end and spin at the correct rate to generate the required centrifugal force. Then another Bola configuration could be added, with the spacecraft touching the previous ones and connected to it with a door or larger opening. This process could continue until a complete torus is

formed. However, small surface area to mass ratio is the biggest disadvantage of this design. Furthermore, this method of growth provides limited space for each module and the lack of variability of offering different g levels in the habitat.

B. Spiral

The idea of spiral structure seems very promising as it offers the easiest possible growth strategy. The growth strategy would just add small increments at the end of the spiral structure. The problem with this notion of growth is that center of mass (CM) of the whole structure changes with growth, so a constant gravity level is not achieved at any local of the habitat. Research to find healthy gravitational levels would likely require constant acceleration levels for a specified period of time. Also a walk down the hall will change you gravity level even without the growth complications.

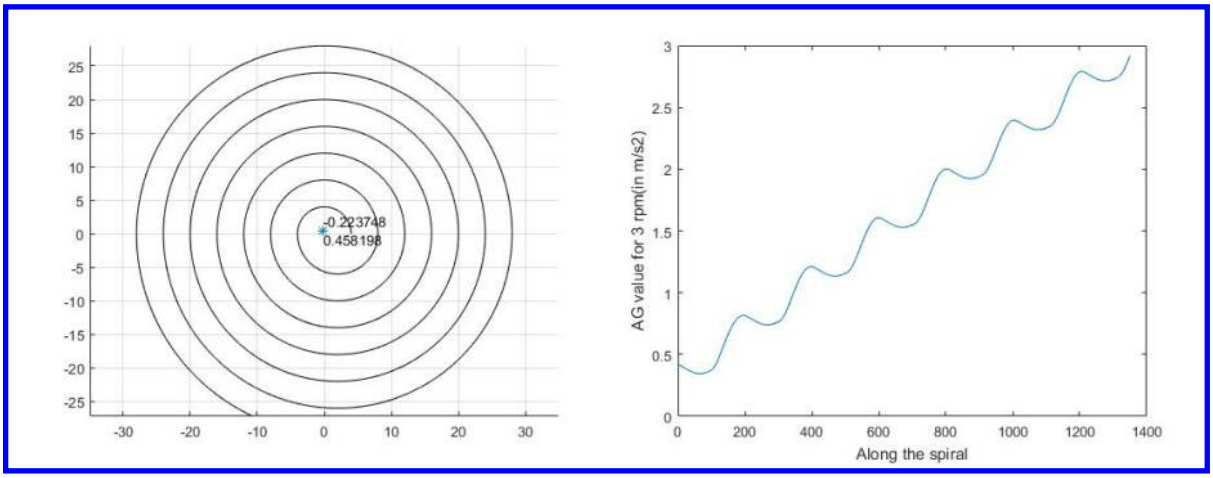

(a) Top view of the spiral (b) AG variation along spiral

Figure 1: Spiral Configuration

It can be observed from the above picture that CM is not at the origin of the spiral. Because of this as people walk along the structure, the effective radius from the CM will change and thus the artificial gravity will also change. One way to solve this issue of moving CM is to add two spirals side by side, with both incrementing in clockwise direction with 180^0 phase apart. This will keep the CM at the origin. The problem with this approach is the changing radius in two spiral configurations will keep changing the CM of cylinders and will cause a wobbling motion about the CM of the whole structure. Hence we dismiss the spiral configuration.

C. Torus

The torus has been a very famous choice among all the ideas to provide artificial gravity in space. The drawbacks of this configuration are the complications of manufacturing, the difficult growth strategy, and the wasted volume, compared to the concentric cylinders described next.

D. Cylinder

Rotating cylinders can be another option to create artificial gravity in space. This seems a very reasonable structure to start with, as it is easy to build and can provide an easy growth strategy. Concentric cylinders can be added without modifying the previous cylinders, except to add an end wall connecting the new cylinder. This method can also provide different g-values at different radii, including a zero-g workshop at the center of rotation (the original cylinder). The concentric circles at the edges of the cylinders allow sections to be joined giving the high stiffness. This adds greater stiffness without adding any mass, compared to the spiral configurations discussed above. For these reasons, we choose the cylindrical approach over the spirals, even though the spirals simplify growth in the radial direction.

III. Growth Strategy

Figure 2 shows the conceptual view of the final space habitat. The blue color overlapping panels show the shield structure required for protection from deep space radiation. Two large half circular plates inclined to both sides of habitat represent the mirrors to provide sunlight into the habitat. The picture also shows a tensegrity robot manufacturing a tensegrity structure for the infrastructure requirement.

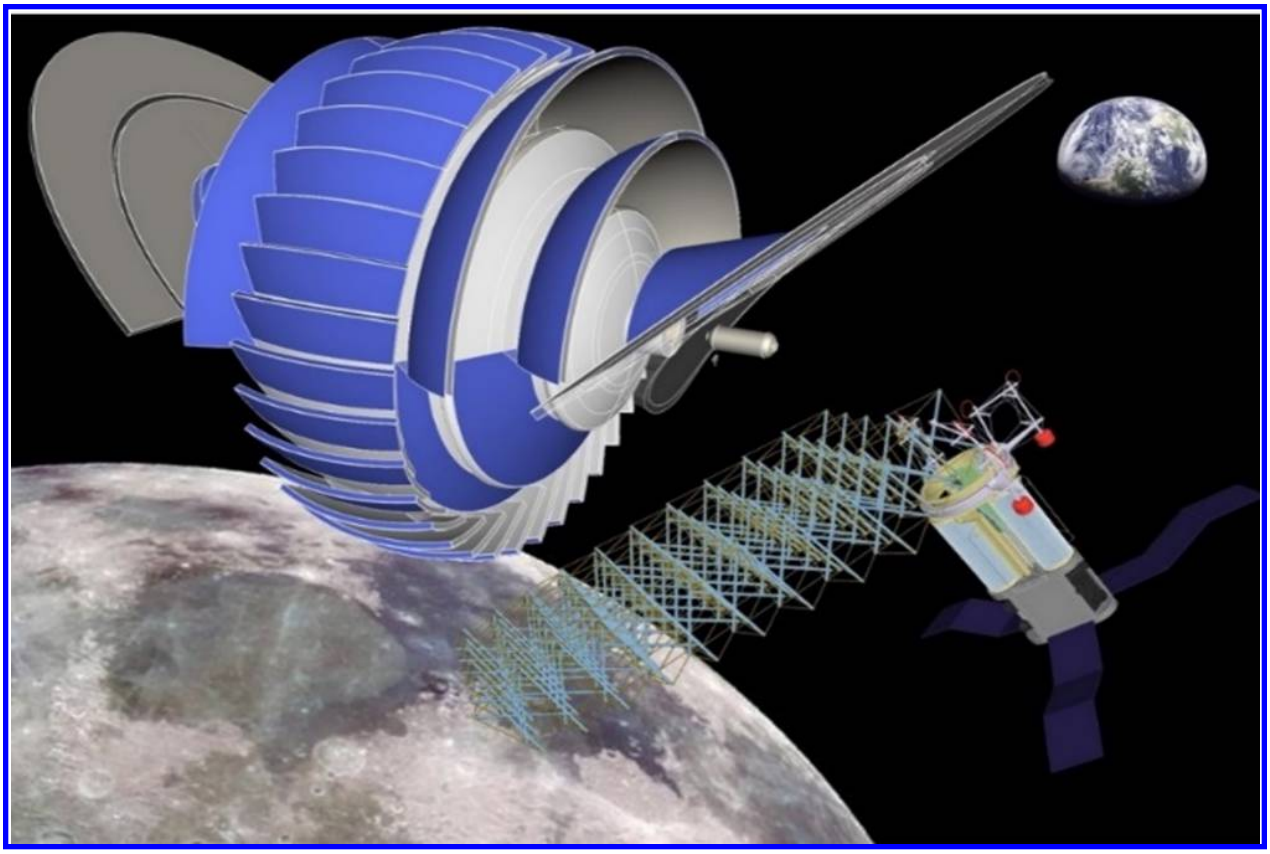

Figure 2: Final conceptual view of Space Habitat with in-space robotic manufacturing

The growth strategy can be easily understood by looking at deployment stages shown in Figure 3-6. Figure 3 shows the cross section view with blue panels around the habitat illustrating the shielding structure. The arrows in the picture represent the sunlight which will bounce back from the shown mirror to provide sunlight into the habitat. The picture also shows the photo-voltaic panels to generate electricity. Green interior part depicts the pressurized environment for humans and agriculture while yellowish area is vacuum between the habitat and the shield. The pink lines represent the cylindrical membrane or the pressure hull to hold the pressure inside. We also have provision for zero gravity workshops for conducting the required experiments to better understand the space.

We start with a simple $40m \times 40m$ (40m length, 40m diameter) circular cylinder. The next growth step can be to add another cylinder of larger radius. Figure 4a shows the assembly of new pressure hull membrane on the shield floor workbench. Tensegrity robots will be used for the laying out of the new floor. As the shield structure would be expanded new pressure hull floor will get stretched enabling lateral stiffness in the membrane. The first hull is already rotating at a certain angular speed to create AG at the surface. Now, the task is to get the new hull to desired radius and rotate it to match the angular speed of the previous cylinder. Powered bogies on the first hull will zero out the relative motion between the new and old hull. A pulling mechanism will set the new hull to its position and then will work as a Mitchell truss structure to provide torsional stiffness in the structure as shown in figure 5a. The next step would be to cut tie-down cables between shield and the new hull. In addition to providing lateral tension in the hull, these cables will also be helpful in controlled motion of the new hull to the prescribed location. In figure 6a, we see a blue pre-rolled window walls that will be unrolled down and zipped to floor to seal the pressurized environment.

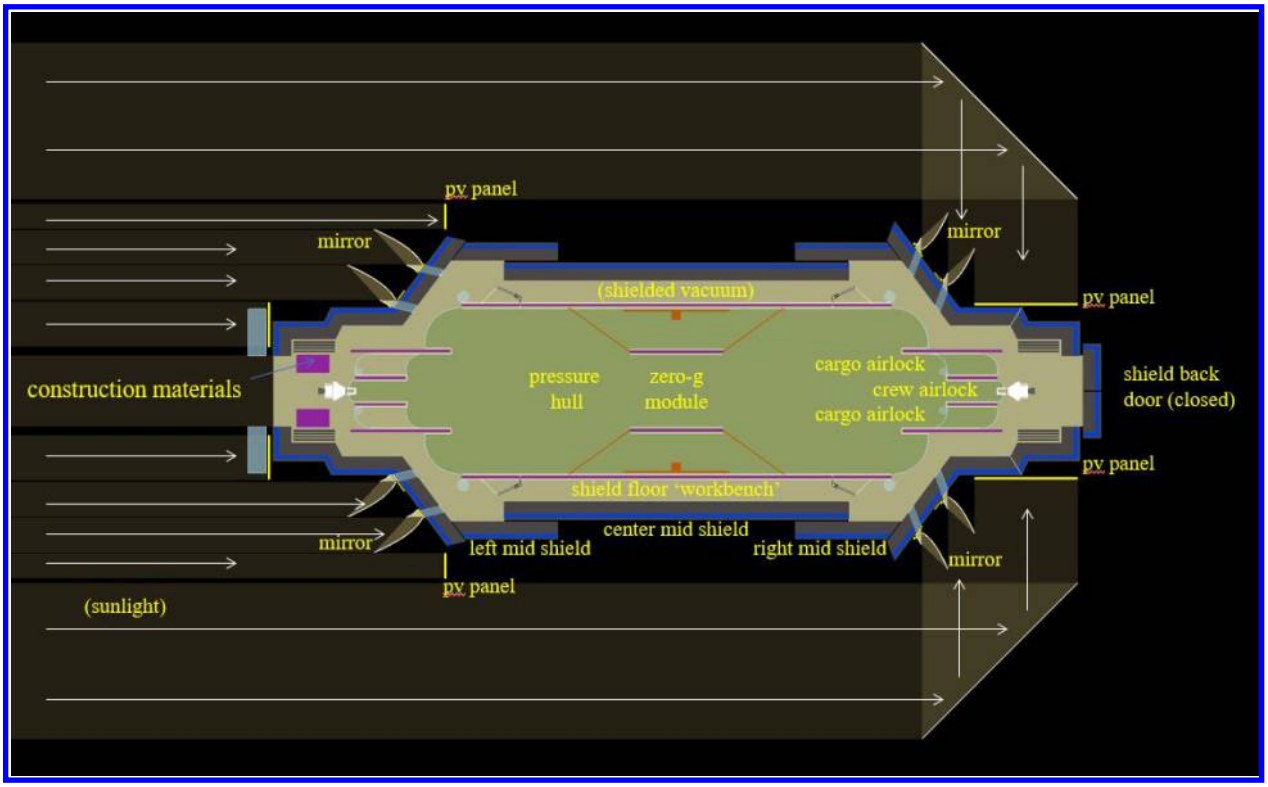

Figure 3: Initial Deployment

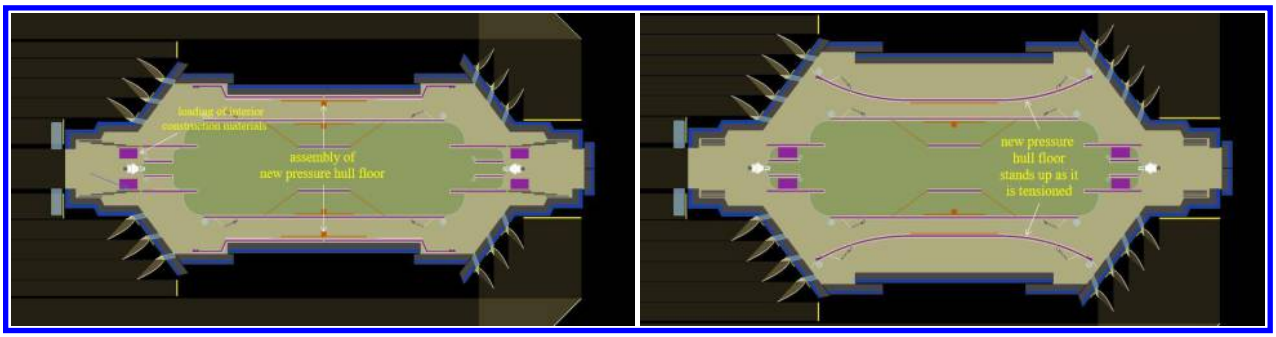

(a) Lateral expansion and floor construction (b) Floor tensioning

Figure 4: Deployment Stages 2-3

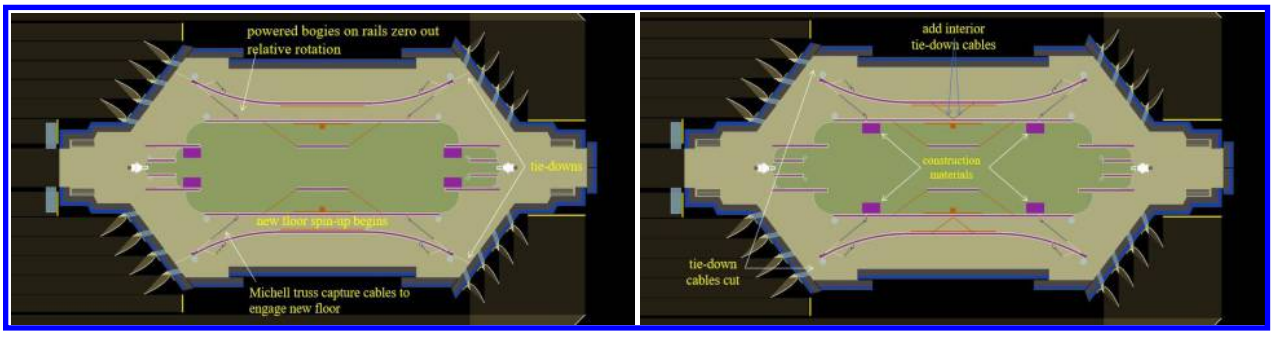

(a) Lateral move and floor capture (b) Cut tie-down cables for new floor

Figure 5: Deployment Stages 4-5

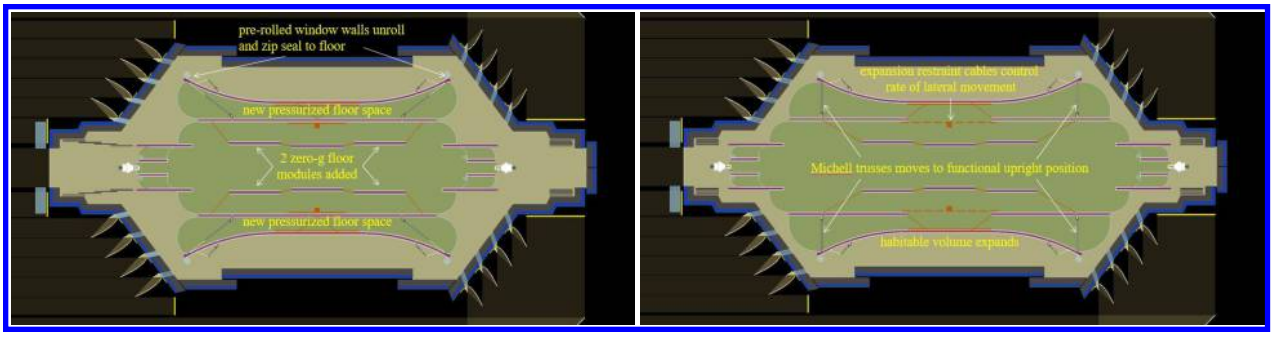

(a) Window walls roll down, seal and pressurize (b) Pressure hull lateral expansion

Figure 6: Deployment Stages 6-7

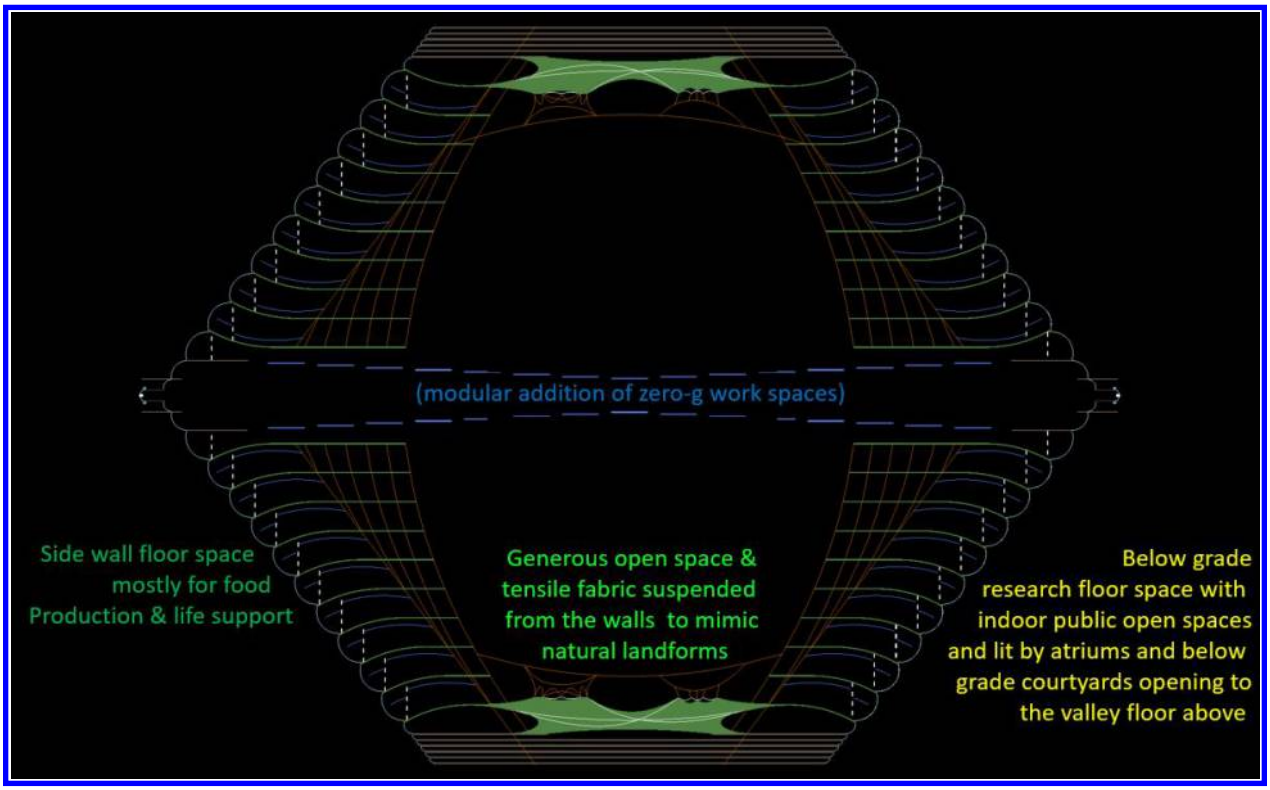

Figure 7: Final stage cross section view of Habitat

The concept is to provide a spacious and livable environment to humans for long term settlement in space. In this regard, we need to cater their need for agriculture and sufficient open space for a happy life. To overcome the problem of congested close cubicles, we can extend the pressure hull laterally to create a big open space in the center of habitat. Figure 6b shows the lateral expansion of the hull with the help of controlled restrained cables to finally yield the cross section of the habitat to figure 7. The green horizontal lines represent the hulls with a zero-g work space in the center of the structure.

IV. Structural Design

The objective of this section is to design a minimum mass cylinder to sustain load due to atmospheric pressure and centrifugal forces while providing required stiffness for any unexpected change in pressure and consequently force. In this regard, we start with a Double-Helix Tensegrity(DHT) structure.[20] A DHT is a

class-2 tensegrity structure with one set of bars following a clockwise pattern and another set of bars following an anti-clockwise pattern. The static analysis shows no need of bars in the DHT cylinder as atmospheric pressure would be providing enough outward force or in other words, would be working as a compressive member. Figure 8 shows the DHT pattern for certain complexity p and q where p is defined as the number of nodes on circular ring and q is the number of circular rings in longitudinal direction, in which all the bars have been replaced by cables. This structure can provide radial and torsional stiffness to the structure due to all the diagonal strings shown in the structure.

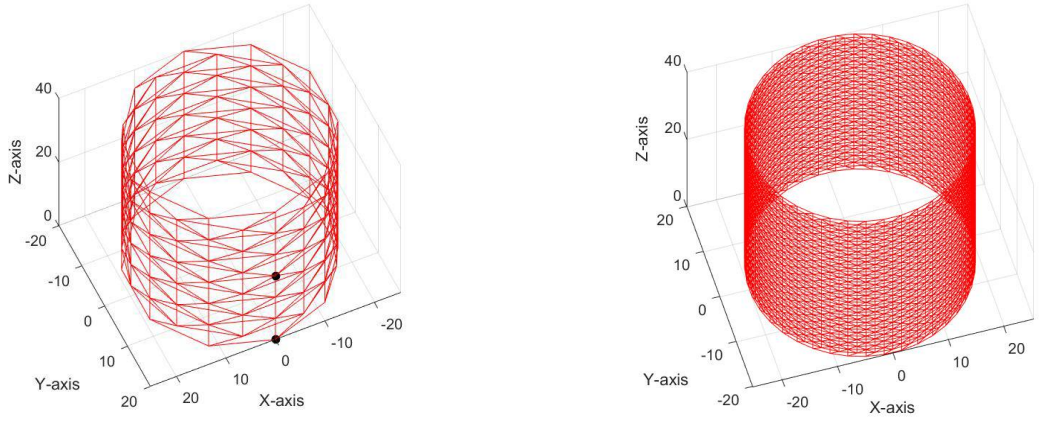

(a) Low complexity (b) High complexity

Figure 8: DHT structure with bars removed (R = 20m and L = 40m)

We need to optimize the complexity of the structure for minimum mass subject to yielding constraint, i.e. we need to find out the optimum number and configuration of the strings in this DHT pattern cylinder to take atmospheric pressure and centrifugal loads.

A. Minimum mass for cable network

Theorem IV.1. *Minimum mass required by a tensegrity string structure to take certain given load and position of nodes is constant, regardless of the configuration or number of strings, provided the configuration is in equilibrium.*

Proof. We know the equilibrium equation for the string cable network for a structure is[21]

$$\begin{aligned} N(C_s^T \hat{\gamma} C_s) &= W \\ N(C_s^T \hat{\gamma} C_s) N^T &= W N^T \\ S \hat{\gamma} S^T &= W N^T. \end{aligned} \tag{1}$$

Now if we look at the minimum mass required for the structure,

$$\begin{aligned} m &= \frac{\rho}{\sigma}[l_1^2 \;\; l_2^2 \;\; l_3^2 ...]\gamma = \frac{\rho}{\sigma}[S_1^T S_1 \;\; S_2^T S_2 \;\; S_3^T S_3 ...]\gamma \\ &= \frac{\rho}{\sigma} \sum_{i=1}^{n} S_i^T S_i \gamma_i = \frac{\rho}{\sigma} \sum_{i=1}^{n} \mathrm{tr}\,(S_i S_i^T)\gamma_i \\ m &= \frac{\rho}{\sigma} \mathrm{tr}\,(S \hat{\gamma} S^T) = \frac{\rho}{\sigma} \mathrm{tr}\,(W N^T). \end{aligned} \tag{2}$$

□

From the above mentioned theorem, it can be easily proven that minimum mass required by this cylinder depends only on the external force matrix W and node position matrix N and does not depend on the

configuration or the arrangement of the strings.

Design considerations for the cylinder: R = 20 m, L = 40 m, Area = 5026 m^2
W = 4 RPM (for 3.51 m/s^2 at the surface), Pressure inside the cylinder = 1 atm (101.325 kpa)
Material used for strings: Spectra (Ultra High Molecular Weight Polyethylene, UHMWPE)
Density: 930 kg/m^3, Yield Strength: 2.1×10^7 N/m^2

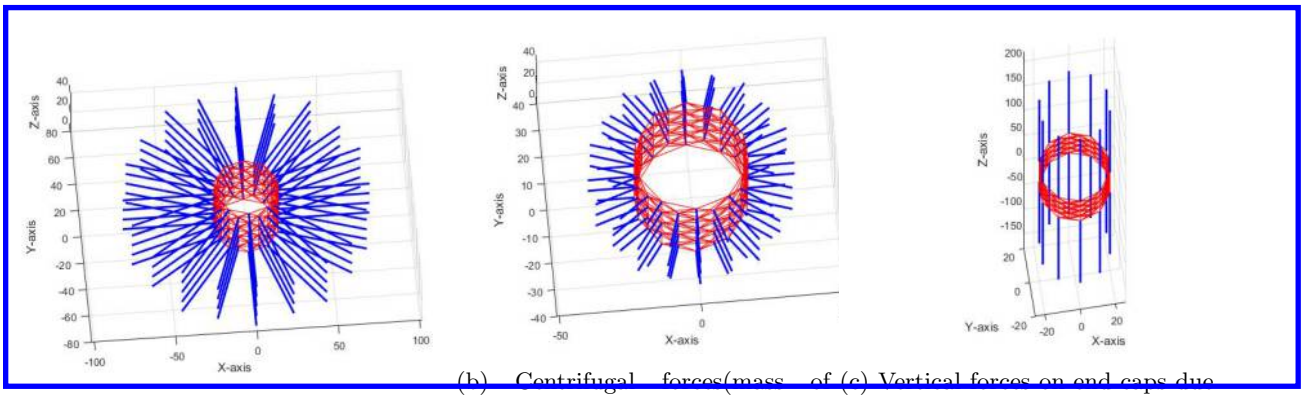

(a) Atmospheric Pressure Forces (b) Centrifugal forces(mass of strings and air inside) (c) Vertical forces on end caps due to pressure

Figure 9: Static Force Analysis

Blue vectors in figure 9a shows the direction and magnitude of forces due to atmospheric pressure. Figure 9b shows the centrifugal forces on nodes due to the mass of strings and mass of the air contained inside the habitat. Finally, there are forces in vertical direction due to the atmospheric pressure on end caps shown in Figure 9c.

From equation 2, we can calculate the minimum mass of the structure to take these loads subject to yielding constraint. Furthermore, it tells us the area of each string in the structure. As the required structure needs to be a membrane to hold the air inside, we design a continuous membrane with different thickness of wires with different orientations derived from the DHT pattern.

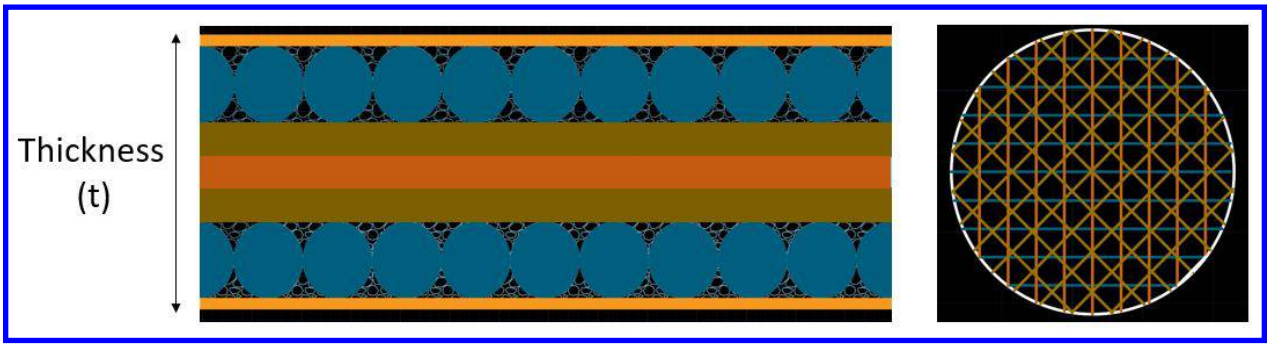

Figure 10: Cross section of membrane

Figure 10 shows 5 layers of wires oriented at different angles. First and last layer is horizontal (0^o), second layer is at 45^o, third layer is vertical (90^o) and fourth layer is aligned at (135^o) with the horizontal. The thickness of the membrane was found to be 5mm for R=20m with a total mass of 1.25×10^4 kg.

However, we need something to stop the relative motion between two concentric cylinders. It is well known that Mitchell configuration[9] described in figure 11 has the minimum mass to take a certain torsional load. Relative rotation between two cylinders is basically because of combination of phase shifted cantilever loads. Thus, adding Mitchell structure seems a good choice here.

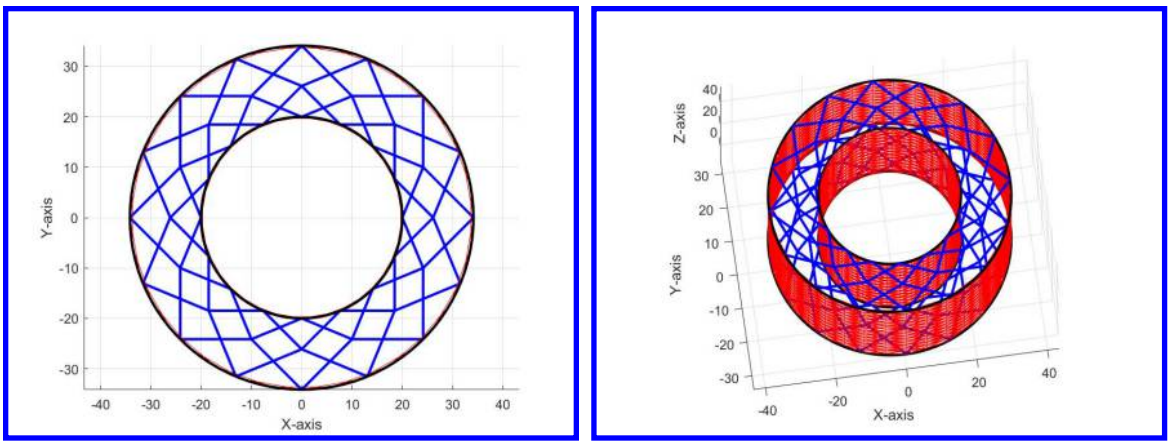

(a) Mitchell Pattern (b) DHT Cylinder with Mitchell

Figure 11: Structure Design with Mitchell Pattern

B. Dynamics of the structure

The study of dynamics of the membrane is important to get the idea of stiffness in the structure. A compact matrix form for the full system dynamics including string masses can be obtained with the following definitions of M_s and K_s.

$$\ddot{N}M_s + NK_s = W \tag{3}$$

$$M_s = \begin{bmatrix} C_{nb}^{\mathrm{T}}(C_b^{\mathrm{T}}\hat{J}_t C_b + C_r^{\mathrm{T}}\hat{m}_b C_r) & C_{ns}^{\mathrm{T}}\hat{m}_s \end{bmatrix} \tag{4}$$

$$K_s = \begin{bmatrix} C_s^{\mathrm{T}}\hat{\gamma}C_{sb} - C_{nb}^{\mathrm{T}}C_b^{\mathrm{T}}\hat{\lambda}C_b & C_s^{\mathrm{T}}\hat{\gamma}C_{ss} \end{bmatrix} \tag{5}$$

where $C_{nb}, C_b, C_{sb}, C_{sb}, C_{ss}$ represent different connectivity matrices for bar to string, string to string and bar to bar nodes as mentioned in our dynamics report.[22]

We use our tensegrity dynamics software to simulate the results. Figure 12 shows the radial and vertical displacement of Bottom point number 3 and Middle point number 43 (shown as black dots in figure 8a) for a step inflation of membrane from its unstretched configuration to final configuration. The mass of individual string has been used from the minimum mass calculation to take the required load. The ratio of unstretched to final length was chosen to provide equilibrium in the final inflated configuration with 1 atmospheric pressure and centrifugal load to get required g-value at the surface.

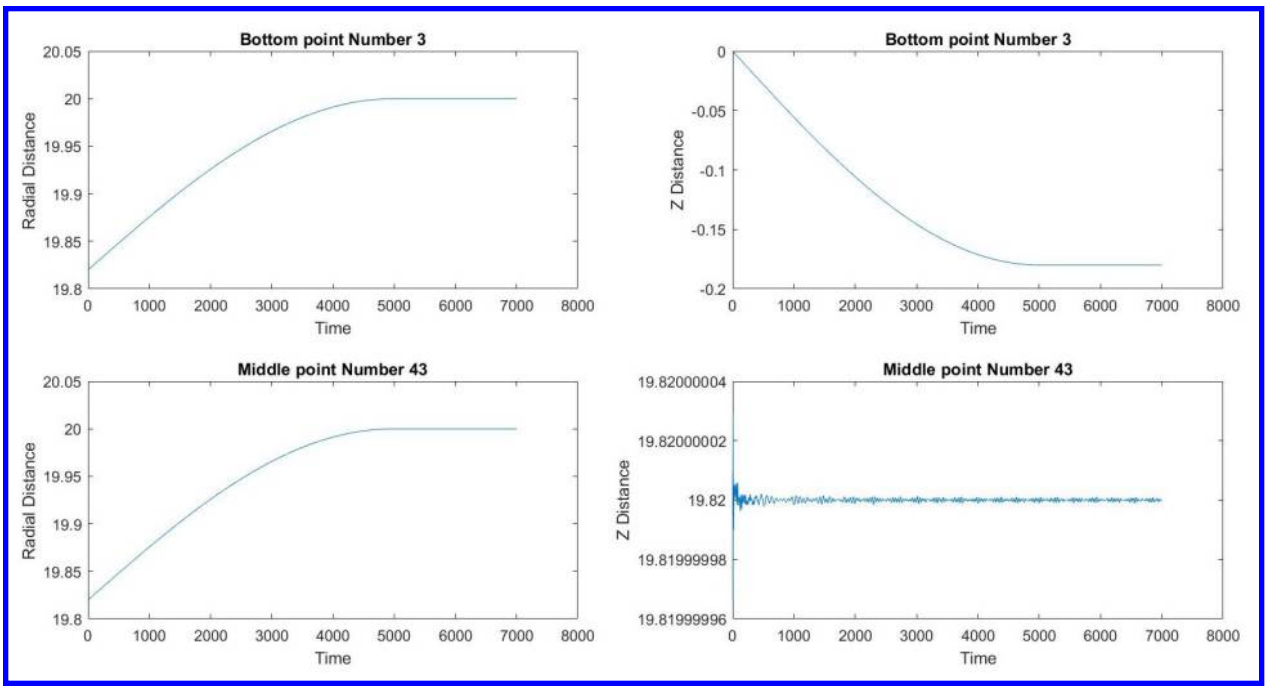

Figure 12: Time history of motion of the certain nodes (R = 20m and L = 40m) for Step Inflation

For the next simulation, we start from the equilibrium position of the structure with 1 atmospheric pressure difference from inside to outside of the cylinder. The stiffness of the individual string is based on the minimum mass calculation. Damping is also added in the strings to get the η (Damping Coefficient) value of 0.1. Figure 13 shows the radial and longitudinal motion of the same nodes of the membrane in presence of 10% instantaneous change in pressure.

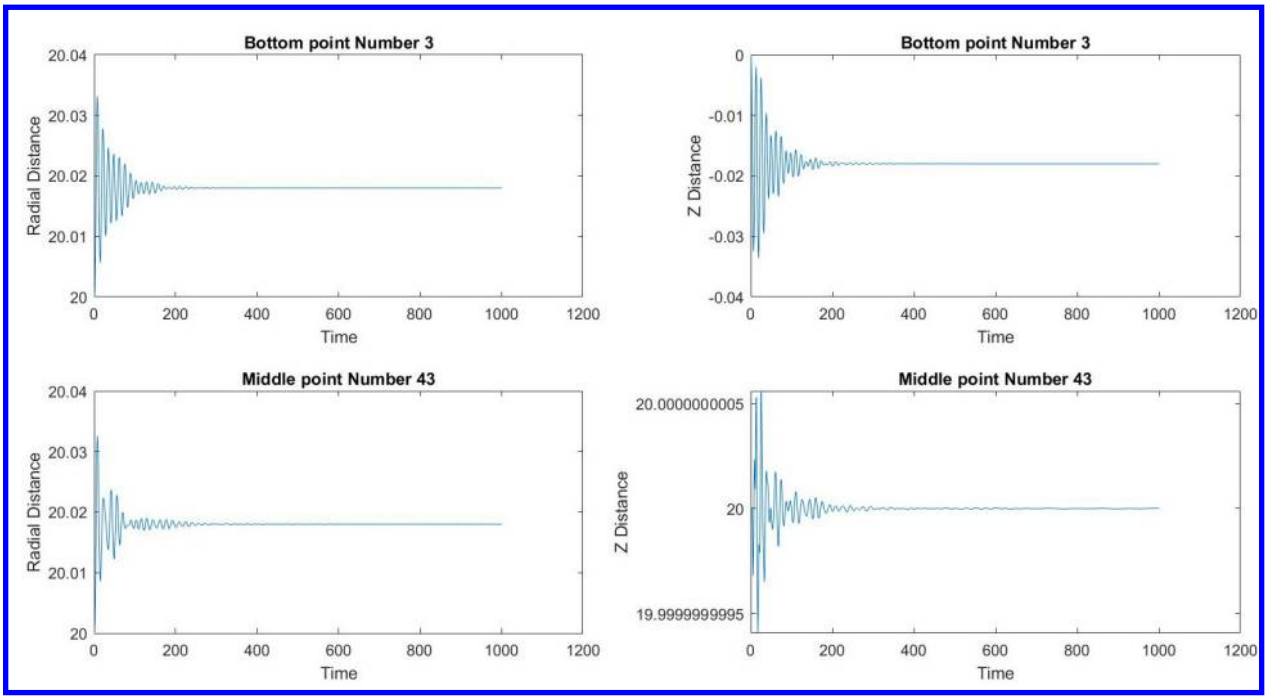

Figure 13: Time history of motion of the certain nodes (R = 20m and L = 40m) for sudden pressure change

The above plot shows less than 4cm change in radial deformation in presence of 10% change in pressure

i.e. 0.2% change in dimension which is acceptable in presence of such an unlikely event.

V. Precession and Attitude Control

One must determine whether the static or dynamic forces dominate the design and stiffness requirements of the structure. Toward this end, we first assume a rigid structure to determine the control forces that would be required if the habitat was a rigid body. These control forces can then (later in our study) be applied to the actual tensegrity flexible habitat to get a first approximation to the impact of dynamics forces, as compared to the static forces that were used in the previous section. This is important since one cannot a priori say which has the greater impact on the design and stiffness requirements of the structure. In other words the design of the structure and the design of the control system are not independent problems.

One may ask whether these goals can be achieved without the use of any control forces. To meet the $1g$-goal, a steady state stable spin about a specific fixed vector in space can be maintained as a stable equilibrium, if the spin axis is aligned with the body's main principal axis (the body is rotating about an axis with the largest inertia). However, control forces are generally required if one seeks to maintain this spin condition in the presence of energy dissipation within the habitat, and/or if one adds the requirement for the spin axis to also follow the sun. The spin about the solar-pointing axis gives the $1g$ and the movement around the sun requires the 360 degrees/year precession.

The control objective is to maintain spin about $\underline{\mathbf{b_2}}$ axis (longitudinal axis of cylinder) to generate required gravity and to get the specific angular velocity about $\underline{\mathbf{e_3}}$ axis (inertial frame) to keep correct precession. These control requirements will provide the necessary angular velocities. Moreover, we also need to add one more objective to keep pointing at sun. As our spin rates are already controlled, we just need to keep $\underline{\mathbf{b_2}}$ in a plane perpendicular to that of $\underline{\mathbf{e_3}}$.

Let us look at the conditions to get correct spin rate and direction. Our desired angular velocity vector is defined as $\underline{\overline{\omega}}$, which is

$$\underline{\overline{\omega}} = \underline{\mathcal{B}}\boldsymbol{\Omega_2}^B + \underline{\mathcal{E}}\boldsymbol{\Omega_3}^E, \tag{6}$$

where

$$\boldsymbol{\Omega_2}^B = [0 \;\; \Omega_2 \;\; 0]^T,$$
$$\boldsymbol{\Omega_3}^E = [0 \;\; 0 \;\; \Omega_3]^T.$$

and Ω_2 is the angular velocity to get required gravity at the surface, Ω_3 is the angular velocity (360 degrees/year) to follow the sun and superscript B and E denote the body and inertial frame respectively. This can be written in body frame as

$$\underline{\overline{\omega}} = \underline{\mathcal{B}}\boldsymbol{\Omega_2}^B + \underline{\mathcal{B}}(\Theta^B)^T\boldsymbol{\Omega_3}^E,$$
$$\overline{\omega}^B = \boldsymbol{\Omega_2}^B + (\Theta^B)^T\boldsymbol{\Omega_3}^E,$$

where $\underline{\mathcal{B}} = \underline{\mathcal{E}}\Theta^B$ and Θ^B represents the direction cosine matrix between body frame and inertial frame. Now, the actual value of the angular velocities in body frame is written as

$$\underline{\omega} = \underline{\mathcal{B}}\omega^B.$$

Therefore, the error in spin rate in body frame can be written as

$$\underline{e_\omega} = \underline{\omega} - \underline{\overline{\omega}},$$
$$e_\omega^B = \omega^B - \boldsymbol{\Omega_2}^B - (\Theta^B)^T\boldsymbol{\Omega_3}^E. \tag{7}$$

Now, this error can be driven to zero using simple first order controller

$$\dot{e_\omega}^B = Ae_\omega^B,$$
$$\dot{\omega}^B - (\dot{\Theta}^B)^T\Omega_3^E = A(\omega^B - \Omega_2^B - (\Theta^B)^T\Omega_3^E)$$
$$\dot{\omega}^B = A(\omega^B - \Omega_2^B - (\Theta^B)^T\Omega_3^E) + (\dot{\Theta}^B)^T\Omega_3^E \tag{8}$$

As mentioned earlier, we also need to keep the $\underline{\mathbf{b_2}}$ axis perpendicular to $\underline{\mathbf{e_3}}$ axis in order to keep pointing at the sun. In other words, the objective is to drive the following error to zero.

$$\begin{aligned} e_\theta &= \underline{\mathbf{b_2}}.\underline{\mathbf{e_3}} \\ &= \underline{\mathcal{B}}[0\ 1\ 0]^T.\underline{\mathcal{E}}[0\ 0\ 1]^T \\ &= \underline{\mathcal{E}}\theta[0\ 1\ 0]^T.\underline{\mathcal{E}}[0\ 0\ 1]^T \\ &= \theta_{32} \\ &= [0\ 0\ 1]^T\Theta[0\ 1\ 0] \\ &= \hat{k}\Theta\hat{j}. \end{aligned} \tag{9}$$

Here, we use second order controller to drive this error to zero

$$\begin{aligned} \ddot{e_\theta} + \alpha\dot{e_\theta} + \beta e_\theta &= 0 \\ \hat{k}\ddot{\Theta}^B\hat{j} + \alpha\hat{k}\dot{\Theta}^B\hat{j} + \beta\hat{k}\Theta^B\hat{j} &= 0 \\ \hat{k}(\dot{\Theta}^B\tilde{\omega}^B + \Theta^B\dot{\tilde{\omega}}^B)\hat{j} + \alpha\hat{k}\dot{\Theta}^B\hat{j} + \beta\hat{k}\Theta^B\hat{j} &= 0 \qquad (\ddot{\Theta}^B = \dot{\Theta}^B\tilde{\omega}^B + \Theta^B\dot{\tilde{\omega}}^B) \\ \hat{k}\Theta^B\dot{\tilde{\omega}}^B\hat{j} &= -\alpha\hat{k}\dot{\Theta}^B\hat{j} - \beta\hat{k}\Theta^B\hat{j} - \hat{k}\dot{\Theta}^B\tilde{\omega}^B\hat{j} \\ (-\theta_{31}\dot{\omega_3} + \theta_{33}\dot{\omega_1}) &= -\alpha\hat{k}\dot{\Theta}^B\hat{j} - \beta\hat{k}\Theta^B\hat{j} - \hat{k}\dot{\Theta}^B\tilde{\omega}^B\hat{j}, \end{aligned} \tag{10}$$

which can be written in terms of $\dot{\omega}$ as

$$[\theta_{33}\ \ 0\ \ -\theta_{31}]\dot{\omega} = -\alpha\hat{k}\dot{\Theta}^B\hat{j} - \beta\hat{k}\Theta^B\hat{j} - \hat{k}\dot{\Theta}^B\tilde{\omega}^B\hat{j}. \tag{11}$$

Now, combining last two equations from above mentioned objectives, we get

$$\begin{bmatrix} \mathbf{I} \\ [\theta_{33}\ 0\ -\theta_{31}] \end{bmatrix}\dot{\omega} = \begin{bmatrix} A(\omega^B - \Omega_2^B - (\Theta^B)^T\Omega_3^E) + (\dot{\Theta}^B)^T\Omega_3^E \\ -\alpha\hat{k}\dot{\Theta}^B\hat{j} - \beta\hat{k}\Theta^B\hat{j} - \hat{k}\dot{\Theta}^B\tilde{\omega}^B\hat{j} \end{bmatrix}. \tag{12}$$

A. Rigid Body Rotation Motion

Angular momentum of a rigid body represented in the body frame is given by

$$\underline{h} = \underline{\mathcal{B}}J^B\omega^B, \tag{13}$$

where J^B and ω^B are the moment of inertia and angular velocity of the body, respectively, both represented in body frame. One can obtain the required torque by taking the inertial derivative of the angular momentum:

$$\underline{\mathcal{B}}T^B = \underline{\dot{\mathcal{B}}}J^B\omega^B + \underline{\mathcal{B}}J^B\dot{\omega}^B. \tag{14}$$

Using ($\underline{\dot{\mathcal{B}}} = \underline{\mathcal{B}}\tilde{\omega}^B$), this can be written as

$$T^B = \tilde{\omega}^BJ^B\omega^B + J^B\dot{\omega}^B. \tag{15}$$

This is the control torque required to make rigid space habitat's attitude error converge to zero.

B. Results

To simulate the results, we assume the rigid body to be a cylinder of radius (R = 20m) and length (L = 40m). We choose the $\underline{\mathbf{b_2}}$ axis of the body frame to be aligned with the longitudinal axis of cylinder and $\underline{\mathbf{e_3}}$ axis of inertial frame to be perpendicular to the ecliptic plane. Initially, the body frame is aligned with the inertial frame. We use spectra (ultra high molecular weight polyethylene, UHMWPE) as the structure material, which has a density of 930 kg/m^3 and a yield strength equal to 2.1×10^7N/m^2. The minimum mass to take these loads constraint to yielding failure is 1.25×10^4 kg.

$$\begin{aligned} R = 20m,\ L = 40m \\ M = 1.25 \times 10^4 Kg \\ J2 = MR^2, J1 = J3 = \frac{1}{2}MR^2 + \frac{1}{12}ML^2 \end{aligned}$$

1. *Simulation I*

This simulation gives us the result with perfect initial conditions.
Initial Condition:

$$\Omega_3 = \pi/(180 \times 24 \times 3600) = 2.02 \times 10^{-7} \text{ (rad/sec)}$$
$$\Omega_2 = \sqrt{g/r} = 0.7004 \text{ (rad/sec)}$$
$$\omega^B(0) = [0\ \Omega_2\ \Omega_3]^T,\ \Theta^B(0) = \mathbf{I}_3$$

Control Parameters:

$$A = -\epsilon\ \mathbf{I}_3 \quad where \quad \epsilon = 1 \times 10^{-3}$$
$$\alpha = 2/5,\ \beta = 2/25$$

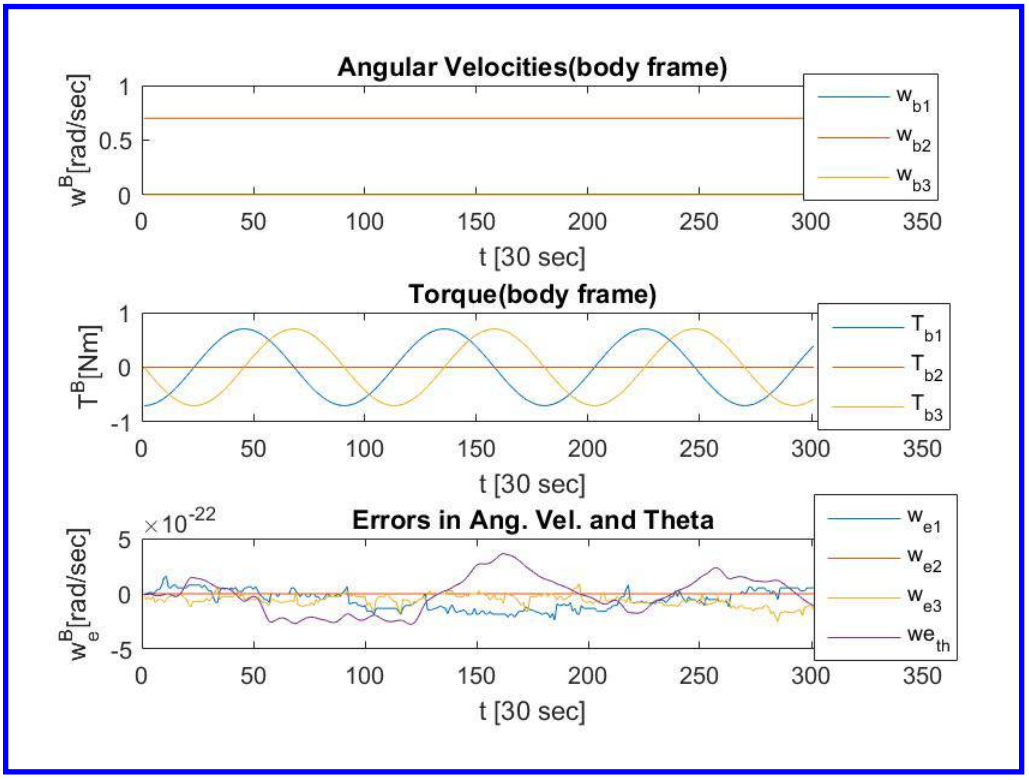

Figure 14: No Initial Error

2. *Simulation II*

In this simulation we start with a small error rate of 1^o/day out of ecliptic plane.
Initial Condition:-

$$\omega^B(0) = [\Omega_3\ \Omega_2\ \Omega_3]^T,\ \Theta^B(0) = \mathbf{I}_3$$

Control Parameters:

$$A = -\epsilon\ \mathbf{I}_3 \quad where \quad \epsilon = 1 \times 10^{-3}$$
$$\alpha = 2/5,\ \beta = 2/25$$

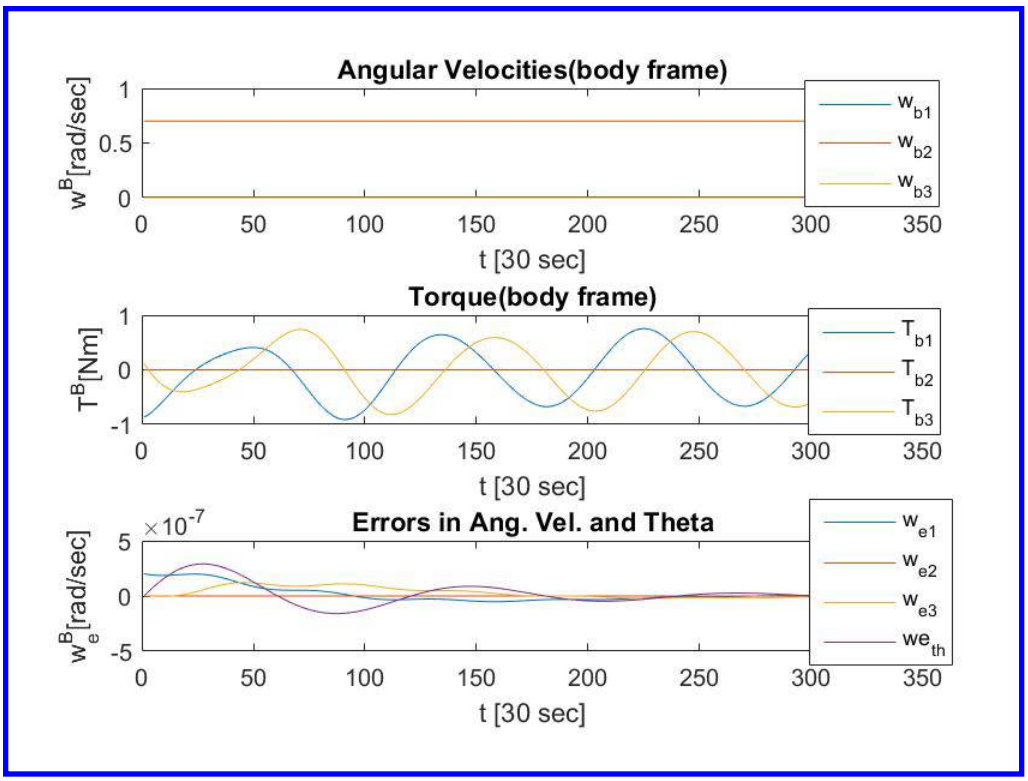

Figure 15: With an initial out of plane error

VI. Conclusion

This paper provides a feasibility study for a growable AG habitat, with shield protection from radiation, and with agriculture space for sustained habitation. The proposed growth strategy sends fabric made on earth and sections are robotically assembled to create a new cylindrical floor and pressurization and rotation steps that match the spin rate of the existing structure. The growth is both radial and longitudinal ia alternate stages of growth. In the structure design, the minimum mass of the structure was found to be independent of the number and configuration of cables within the UHMWPE material. The dynamic simulation results were shown for inflation transients inside the pressure hull. The growth continues to 225m radius at which the gravity gradient is 1%. The habitat provides all levels of gravity from zero-g to 1-g, where the lower g-level space is reserved for agriculture and the humans occupy higher g-levels up ti 1-g. An attitude and angular velocity control scheme is proposed to manage the spin rate and attitude of this habitat in such a way that both gravity and sunlight requirements are met. The performance of this control algorithm is simulated using numerical simulations.

References

[1]Hall, T. W., "ARTIFICIAL GRAVITY AND THE ARCHITECTURE OF ORBITAL HABITATS," *Journal of the British Interplanetary Society*, Vol. 52, July/August 1999, pp. 290–300.

[2]Hall, T. W., "Artificial Gravity Visualization, Empathy, and Design," *AIAA Space 2006*, 2006.

[3]Keller TS, Strauss AM, S. M., "Prevention of bone loss and muscle atrophy during manned space flight," *Microgravity Quarterly*, Vol. 2(2), April 1992, pp. 89–102.

[4]Diamandis, P. H., "Reconsidering Artificial Gravity for Twenty-First Century Space Habitats," *Space Manufacturing 6 - Nonterrestrial Resources, Biosciences, and Space Engineering: Proceedings of the Eighth Princeton / AIAA / SSI Conference*, 1987, pp. 55–68.

[5]Johnson, H., "Space settlements:a design study,," *National Aeronautics and Space Administration*, 1977.

[6]Young, L. R., Yajima, K., and Paloski, W. E., "Artificial Gravity Research to Enable Human Exploration," *International Academy of Astronautics, Paris, France*, September 2009.

[7]Skelton, R. and Longman, A., "Growth capable tensegrity structures as an enabler of space colonization," *AIAA Space 2014 Conference and Exposition*, 2014, p. 4370.

[8]Kennedy, K., "Lessons from TransHab: An Architect's Experience," *AIAA Space Architecture Symposium. Houston, Texas*, 2002.

[9]Skelton, R. and de Oliveira, M., *Tensegrity Systems*, Springer US, 2009.

[10]Fuller, R., Applewhite, E., and Loeb, A., *Synergetics; explorations in the geometry of thinking*, Macmillan, 1975.

[11]Lalvani, H., "Origins Of Tensegrity: Views Of Emmerich, Fuller And Snelson," *International Journal of Space Structures*, Vol. 11, No. 1-2, 1996, pp. 27.

[12]Skelton, R. E. and de Oliveira, M. C., "Optimal complexity of deployable compressive structures," *Journal of the Franklin Institute*, Vol. 347, No. 1, 2010, pp. 228–256.

[13]Skelton, R. E. and de Oliveira, M. C., "Optimal tensegrity structures in bending: The discrete Michell truss," *Journal of the Franklin Institute*, Vol. 347, No. 1, 2010, pp. 257–283.

[14]Skelton, R. E., Montuori, R., and Pecoraro, V., "Globally stable minimal mass compressive tensegrity structures," *Composite Structures*, Vol. 141, 2016, pp. 346–354.

[15]Djouadi, S., Motro, R., Pons, J. C., and Crosnier, B., "Active Control of Tensegrity Systems," *Journal of Aerospace Engineering*, Vol. 11, No. 2, 1998, pp. 37–44.

[16]Hagiwara, Y. and Oda, M., "Transformation experiment of a tensegrity structure using wires as actuators," *Mechatronics and Automation (ICMA), 2010 International Conference on*, 2010, pp. 985–990.

[17]Koizumi, Y., Shibata, M., and Hirai, S., "Rolling tensegrity driven by pneumatic soft actuators," *Robotics and Automation (ICRA), 2012 IEEE International Conference on*, 2012, pp. 1988–1993.

[18]Motro, R., "Structural morphology of tensegrity systems," *Meccanica*, Vol. 46, No. 1, 2011, pp. 27–40.

[19]Paul, C., Valero-Cuevas, F. J., and Lipson, H., "Design and control of tensegrity robots for locomotion," *IEEE Transactions on Robotics*, Vol. 22, No. 5, 2006, pp. 944–957.

[20]Nagase, K. and Skelton, R. E., "Double-Helix Tensegrity Structures," *AIAA Journal*, Vol. 53, No. 4, 2014, pp. 847–862.

[21]Cheong, J. and Skelton, R. E., "Nonminimal Dynamics of General Class k Tensegrity Systems," *International Journal of Structural Stability and Dynamics*, Vol. 15, No. 2, 2015, pp. 1450042 (22 pages).

[22]James V Henrickson, Raman Goyal, R. E. S., "Class K Tensegrity System Dynamics with Massive Strings and Elastic Skin," *Texas A&M University*, 2017.